Progressive Inhibition by Water Deficit of Cell Wall Extensibility and Growth along the Elongation Zone of Maize Roots Is Related to Increased Lignin Metabolism and Progressive Stelar Accumulation of Wall Phenolics[1]

Ling Fan, Raphael Linker, Shimon Gepstein, Eiichi Tanimoto, Ryoichi Yamamoto, and Peter M. Neumann*

Plant Physiology Laboratory, Department of Environmental, Water, and Agricultural Engineering, Faculty of Civil and Environmental Engineering (L.F., R.L., P.M.N.) and Faculty of Biology (S.G.), Technion-Israel Institute of Technology, Haifa 32000, Israel; Plant Physiology Laboratory, Department of Information and Biological Sciences, Graduate School of Natural Sciences, Nagoya City University, Nagoya 467–8501, Japan (E.T.); and Biology and Chemistry Laboratory, Tezukayama University, Nara 631–8585, Japan (R.Y.)

Water deficit caused by addition of polyethylene glycol 6000 at −0.5 MPa water potential to well-aerated nutrient solution for 48 h inhibited the elongation of maize (*Zea mays*) seedling primary roots. Segmental growth rates in the root elongation zone were maintained 0 to 3 mm behind the tip, but in comparison with well-watered control roots, progressive growth inhibition was initiated by water deficit as expanding cells crossed the region 3 to 9 mm behind the tip. The mechanical extensibility of the cell walls was also progressively inhibited. We investigated the possible involvement in root growth inhibition by water deficit of alterations in metabolism and accumulation of wall-linked phenolic substances. Water deficit increased expression in the root elongation zone of transcripts of two genes involved in lignin biosynthesis, cinnamoyl-CoA reductase 1 and 2, after only 1 h, i.e. before decreases in wall extensibility. Further increases in transcript expression and increased lignin staining were detected after 48 h. Progressive stress-induced increases in wall-linked phenolics at 3 to 6 and 6 to 9 mm behind the root tip were detected by comparing Fourier transform infrared spectra and UV-fluorescence images of isolated cell walls from water deficit and control roots. Increased UV fluorescence and lignin staining colocated to vascular tissues in the stele. Longitudinal bisection of the elongation zone resulted in inward curvature, suggesting that inner, stelar tissues were also rate limiting for root growth. We suggest that spatially localized changes in wall-phenolic metabolism are involved in the progressive inhibition of wall extensibility and root growth and may facilitate root acclimation to drying environments.

Water deficit occurs in drying environments when water uptake via the plant root system cannot meet water requirements for unrestricted growth, photosynthesis, and transpiration in the shoots. Water deficit can reduce root growth, shoot growth, and crop yields on a world wide scale (Boyer, 1982). Ongoing root growth is required to facilitate water and nutrient uptake from the soil, and therefore, there is much interest in the mechanisms by which root growth is regulated in general and inhibited under water deficit (Sharp et al., 1988; Sinclair and Muchow, 2001; Dolan and Davies, 2004). Growth of individual roots is known to be driven by the irreversible elongation of daughter cells continuously produced by dividing cells in the apical meristem. Cell elongation is driven by the interaction between turgor pressure and the regulated yielding of the expanding cell walls.

In maize (*Zea mays*) primary roots, cell production, final cell length, the length of the root elongation zone, and overall root elongation rates are all reduced under water deficit (Fraser et al., 1990; Pritchard, 1994). Segmental analysis of growth rates along the root elongation zone under well-watered conditions reveals accelerating growth rates up to 4 mm behind the tip, followed by the onset of decreasing rates of elongation until growth ceases, approximately 10 mm behind the tip. Similar spatial patterns of growth distribution have been observed in Arabidopsis (*Arabidopsis thaliana*) roots and may be universal for flowering plants (Van der Weele et al., 2003). Under water deficit, root segmental elongation rates are surprisingly well maintained in the accelerating region but are progressively inhibited (by comparison with well-watered controls) in adjacent regions approximately 3 to 9 mm behind the tip (Sharp et al., 1988; Pritchard, 1994; Fan and Neumann, 2004).

Micropressure probe measurements indicated that turgor pressures remain fairly constant along and beyond the length of the elongation zone of maize roots under well-watered and water deficit conditions, despite the segmental variation in growth rates (Spollen and Sharp, 1991; Pritchard, 1994). Turgor differences

[1] This work was supported by FMW chair and Manlam (grant to P.M.N.) and a Zeff Fellowship (to R.L.).

* Corresponding author; e-mail agpetern@tx.technion.ac.il; fax 972–4–8228898.

The author responsible for distribution of materials integral to the findings presented in this article in accordance with the policy described in the Instructions for Authors (www.plantphysiol.org) is: Peter M. Neumann (agpetern@tx.technion.ac.il).

Article, publication date, and citation information can be found at www.plantphysiol.org/cgi/doi/10.1104/pp.105.073130.

did not therefore appear to be responsible for variation in growth rates. Instead, spatially selective effects of water deficit on the extension capacity of expanding root cell walls appeared to be involved (e.g. Pritchard et al. 1993; Neumann et al., 1994; Wu et al., 1996).

The mechanisms involved in regulating cell wall extension capacity and hence growth in roots (and elsewhere in plants) remain the subject of intensive investigation and frequent review (e.g. Taiz, 1984; Masuda, 1990; Rayle and Cleland, 1992; Neumann, 1995; Carpita, 1996; Yamamoto, 1996; Cosgrove, 2000; Carpita and McCann, 2002; Birnbaum et al., 2003; Bassani et al., 2004; Dolan and Davies, 2004; Fry, 2004; Passardi et al., 2004; Rose et al., 2004; Sharp et al., 2004). Complex multigenic interactions involving load-bearing wall polysaccharides, phenylpropanoids, peroxidases, reactive oxygen species, calcium ions, wall proteins such as extensins or expansins, wall enzymes such as xyloglucan endotransglucosylases, and proton pumping into the wall have all been indicated. For example, Fan and Neumann (2004) reported that the remarkable maintenance of wall extensibility and segmental growth rates in the region 0 to 3 mm behind the tip of maize primary roots under water deficit was associated with root capacity to maintain an acidic cell wall pH (pH 5.2) and that the accompanying inhibition by water deficit of segmental growth rates in the region 3 to 9 mm behind the root tip was associated with comparatively reduced wall acidification. However, growth in the 3-to-6-mm region was only partially restored by exogenous acidification to pH 4.5 while in the 6-to-9-mm region, growth was not increased. Thus, additional growth inhibitory factors were apparently involved. Wu et al. (1996) also showed an absence of acid pH effects on extension characteristics of isolated root cell walls from the basal elongation zone of water-stressed roots. We became interested in the possibility that water deficit might act to locally alter the composition of cell walls in the basal region of the root elongation zone, thereby reducing wall extensibility, responsiveness to acid pH, and root growth.

Maize has type 2 cell walls, which are composed of proteins, cellulose microfibrils, glucuronoarabinoxylans of varying degrees of side group substitution, and mixed-linkage β-glucans. These are interwoven with a complex three-dimensional network of cross-linking phenylpropanoids (Carpita et al., 2001; Carpita and McCann, 2002). Several reports suggest that cell wall binding of phenolic substances, for example as oxidatively linked Tyr bridges between wall structural proteins, di or tri ferulic ester bridges between wall arabinoxylan polymers, or as more complex lignin polymer deposits, may be associated with wall stiffening during cell maturation (e.g. Fry, 1979, 1986; Kamisaka et al., 1990; Ralph et al., 1995; Carpita, 1996; Degenhardt and Gimmler, 2000; Schopfer et al., 2001; MacAdam and Grabber, 2002; Boerjan et al., 2003; Jung, 2003; Fry, 2004). However, the hypothesis that progressive inhibition by water deficit of wall extensibility and segmental growth rates in the root elongation zone may be related to spatially localized and progressive alterations in patterns of wall-phenolic accumulation, does not appear to have been previously investigated.

We reasoned that maize root tissues grow at comparable rates from 0 to 3 mm behind the tip under control and water deficit conditions, while the growth-inhibitory developmental changes induced by water deficit begin to take effect in the region situated 3 to 9 mm behind the tip. We therefore investigated changes in metabolism and accumulation of cell wall-linked phenolic substances and the progressive inhibition by water deficit of wall extensibility and growth rates in this region.

Lignin is well known as a phenolic compound involved in reducing wall extensibility. Moreover, enzymes such as cinnamoyl-CoA reductase (CCR, EC 1.2.1.44) are active at the entry point to the monolignol-specific branch of the lignin biosynthetic pathway in maize and other species (Pichon et al., 1998; Boerjan et al., 2003). We therefore used a candidate gene approach with semiquantitative reverse transcription (RT)-PCR and northern blots to investigate the possible expression of transcripts of lignin synthesis genes and the time scale of effects of water deficit thereon, in the maize root elongation zone. In addition, possible stress-induced changes in levels of cell wall-bound phenolics, carbohydrates, and proteins at specific locations along the root elongation zone and beyond were investigated by Fourier transform infrared (FTIR) spectroscopy (Séné et al., 1994; Carpita and McCann, 2002). The localized accumulation of cell wall-bound phenolics, under well-watered or water deficit conditions, was then visualized in cross sections from equivalent root regions using UV-fluorescence microscopy (Harris and Hartley, 1976; Rudall and Caddick, 1994) and by in situ staining for lignins (Chapple et al., 1992). Finally, we used a surgical approach to determine whether localized accumulation of wall phenolics occurred in the root tissues, which actually limited root elongation.

RESULTS

Effects of Polyethylene Glycol 6000-Induced Water Deficit on Root Growth Parameters

Water deficit is known to cause reductions in cell size and differential changes in segmental growth rates and wall extensibility along the approximately 10-mm long elongation zone at the apex of maize primary roots. We added a nonpenetrating osmoticum, polyethylene glycol (PEG) 6000 (at -0.5 MPa water potential) to the well-aerated nutrient medium to impose a 48-h water deficit on maize seedlings. After 48 h under these conditions, rates of root elongation were quasi-linear and approximately half that of well-watered control roots (Fan and Neumann, 2004). The comparative reductions in root segmental elongation rates induced by water deficit in the regions

0 to 3, 3 to 6, and 6 to 9 mm behind the tip were 0%, 57%, and 93%, respectively. Elongation rates were zero at distances greater than 10 mm from the tip. Note that the inhibition of segmental growth rates induced by water deficit was only initiated as expanding root cells, which traverse the elongation zone in a matter of hours, entered the still-elongating regions 3 to 6 mm behind the tip. Thus, we considered them to be of near-equivalent developmental status at this location.

The mean lengths of fully elongated cortical cells were also reduced, from 0.238 ± 0.002 mm for unstressed controls to 0.157 ± 0.001 mm under water deficit (means ± SE, $n = 210$). The progressively increasing inhibition by water deficit of root segmental growth rates along the region 3 to 9 mm behind the tip was associated with significant ($P = 0.05$) reductions in comparative mechanical extensibility (assayed at pH 4.6 to maximize wall loosening) of cell walls in alcohol-extracted root tissue segments from the same region. Thus, wall extensibility in the 3-to-6-mm region, where growth inhibition was initiated, was reduced from 0.219 ± 0.003 mm mm^{-1} in well-watered controls to 0.199 ± 0.005 mm mm^{-1} under water deficit (means ± SE, $n \geq 15$). Extensibility at 6 to 9 mm from the tip was reduced from 0.198 ± 0.005 mm mm^{-1} in control roots to 0.148 ± 0.004 mm mm^{-1} under water deficit. These progressive decreases were presumably independent of pH limitations and likely involved wall stiffening by chemical bonding of wall polymers. Importantly, no equivalent reductions in wall extensibility were detected after only 1 h of water deficit.

Having established that our water deficit regime resulted in spatially localized root growth responses similar to those previously reported by others, we proceeded to investigate the possible involvement of cell wall phenolics in these responses.

Water Deficit Increases Transcript Levels of CCR1 and CCR2 Genes in the Root Elongation Zone

CCR1 and CCR2 are important genes in the biochemical pathways of lignin biosynthesis. Using a candidate gene approach, PCR amplification, and northern-blot assays (as described in "Materials and Methods") we detected basal levels of CCR transcript expression in the elongation zone of control roots. These were up-regulated after 1 and 48 h of water deficit treatment as shown by the CCR1 and CCR2 amplicons and the related bar graph, which shows the progressive increases in ratio-corrected (in comparison with 18S RNA) pixel densities for each PCR product after 1 or 48 h of water deficit (Fig. 1A). The CCR products of the PCR appeared in the expected positions on the gel, and when sequenced they showed 96% and 100% homology to equivalent sequences in the gene database for CCR1 and CCR2, respectively. Similar stress-induced increases in CCR transcript expression were revealed by the northern-blot analyses (Fig. 1B). Thus, transcripts of genes involved in biosynthesis of lignin from its phenolic precursors were expressed within the root elongation zones of well-watered roots and of roots under water deficit. Since transcript levels were up-regulated within 1 h of imposition of water deficit and before measurable changes in wall extensibility, they may be causally related to changes in wall lignin deposition, which could stiffen the wall and reduce its extensibility. We have not yet determined the spatial distribution of CCR gene transcripts. However, direct evidence for localized effects of water deficit on accumulation in the root elongation zone of cell wall phenolics and lignin was provided by IR, UV, and lignin staining.

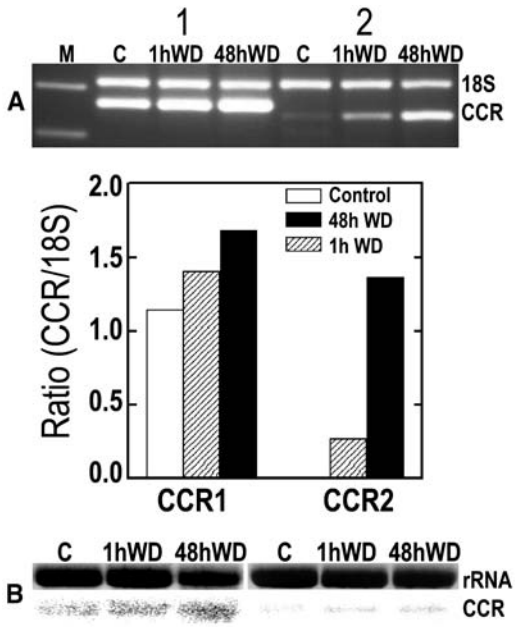

Figure 1. Water deficit (WD) for 1 and 48 h increases the transcript levels of CCR genes in the root elongation zone as compared with well-watered controls (C). A, Relative RT-PCR analyses; lane M shows markers of 200 and 300 bp; 18S indicates a 315-bp fragment of 18S ribosomal RNA used as the internal standard; first three lanes after marker lane are for CCR1 amplicon (263 bp); next three lanes are for CCR2 amplicon (242 bp). The bar graph shows the progressive increases in ratio-corrected (by comparison with 18S RNA) pixel densities for each PCR product after 1 or 48 h of water deficit. Ratio value for CCR2 control is too small to appear. B, Similar water deficit-induced increases in CCR1 and CCR2 transcript levels shown by RNA gel-blot hybridization analysis.

Water Deficit Causes Spatial Changes in Cell Wall Composition

FTIR spectral analyses were performed on root cell walls that were repeatedly alcohol extracted to ensure relative freedom from interference by soluble contaminants. To establish the segmental distribution of stress-induced cell wall changes, FTIR spectra were collected in the mid-IR range for separate batches of cell wall material from 0 to 3, 3 to 6, 6 to 9, and 9 to 12 mm behind the root tip. The left-hand side of Figure 2 shows FTIR spectra at 2,000 to 800 cm^{-1} for cell wall material from water deficit treated (upper spectrum) and control roots. The arrow (Fig. 2, a) marks a typical

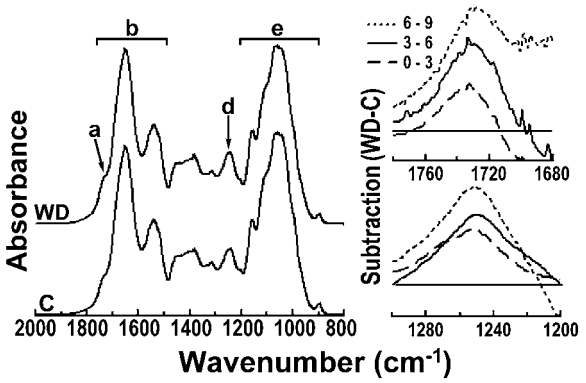

Figure 2. FTIR absorbance differences between cell walls from water deficit-treated and control roots at increasing distances from tip. Left-hand figure shows average FTIR absorbance spectra over the 2,000 to 800 cm^{-1} range for cell walls of control roots (C) and roots under water deficit (WD) from the region 6 to 9 mm behind the root tip. The spectra were baseline corrected and area normalized. The arrow (a) marks a shoulder in the 1,740 to 1,720 cm^{-1} region, which is indicative for alkyl and phenyl esters. Horizontal bar (b) emphasizes major bands indicative of amide I and amide II. The arrow (d) points to absorbance around 1,245 cm^{-1}, which is indicative of C-O-H deformation and C-O stretching of phenols plus asymmetric C-C-O stretching of esters (Séné et al., 1994). The bar (e) indicates carbohydrate absorbance bands. Mean spectra based on separate assays of six batches of roots. Difference spectra on the right side of the figure were generated by digital subtraction of the spectral absorbance values of control root cell wall preparations between 1,780 and 1,680 cm^{-1} (in top figure) and between 1,200 and 1,300 cm^{-1} (in bottom figure) from corresponding absorbance values for walls of water deficit-treated roots. Key in top right-hand figure differentiates the subtraction plots for cell walls from 0 to 3, 3 to 6, and 6 to 9 mm behind the tip. Note progressive increases induced by water deficit in phenol-related absorbance at 1,720 to 1,740 cm^{-1} and at 1,245 cm^{-1} as distances from tip increase. No further increases were measured at 9 to 12 mm from tip. Horizontal lines represent zero difference between treatments at indicated wave numbers along the *x* axis.

shoulder in the 1,720 to 1,740 cm^{-1} region, which is indicative for alkyl and phenolic esters. The horizontal bar (Fig. 2, b) emphasizes major bands indicative of amide I and amide II. The arrow (Fig. 2, d) points to an absorbance band around 1,245 cm^{-1}, which also suggests phenolic and ester groupings. The bar (Fig. 2, e) indicates carbohydrate absorbance bands (Séné et al., 1994).

The FTIR spectra were statistically analyzed for possible differences induced by water deficit using principal component analysis (PCA). Exploratory PCA was able to detect significant differences between cell wall spectra from water deficit and control treatments only in the 1,800 to 1,600 cm^{-1} region surrounding the 1,720 to 1,740 cm^{-1} shoulder and in the 1,260 to 1,220 cm^{-1} region surrounding the 1,245 cm^{-1} peak. These treatment-induced differences appeared in each of the root regions that were investigated and are indicated by the separation between white and black symbols in Figure 3, A and B, respectively. Thus, water deficit induced statistically significant differences in the phenolic absorbance of cell wall material along the entire root elongation zone, while carbohydrate and amide (protein) absorbance did not appear to change.

The progressive effects of water deficit on the absorbance of phenolics and esters in walls from different regions along the root elongation zone were clearly revealed by digital subtraction of appropriate spectral absorbance values for nonstressed roots from spectral absorbance values of equivalent regions in roots under water deficit. The difference spectra for 1,780 to 1,680 cm^{-1} and for 1,300 to 1,200 cm^{-1} are shown in separate plots on the right-hand side of Figure 2. The plots reveal the progressive increases in absorbance (points above the horizontal zero line) that were induced by the water deficit treatment at increasing distances from the tip (0–3, 3–6, and 6−9 cm) and at two independent sets of wave numbers associated with wall phenolic and ester linkages, i.e. 1,720 to 1,740 cm^{-1} and 1,245 cm^{-1}. The mean absorbance difference at 1,720 cm^{-1} progressively increased from 0.75 ± 0.60 cm^{-1} at 0 to 3 cm from the tip to 2.34 ± 0.37 cm^{-1} at 3 to 6 cm and 3.93 ± 1.16 cm^{-1} at 6 to 9 cm. Similarly, absorbance difference at 1,245 cm^{-1} progressively increased from 1.63 ± 0.32 cm^{-1} at 0 to 3 cm from the tip to 2.19 ± 0.11 cm^{-1} at 3 to 6 cm and 2.98 ± 0.26 cm^{-1} at 6 to 9 cm (means ± SE, $n = 6$).

The water deficit-induced increase in absorbance of phenolics at 6 to 9 cm from the tip was spatially associated with the region of greatest root growth inhibition by water deficit. The increases in this region might be caused by direct stress effects on development or as a developmental result of stress-induced and premature cessation of elongation. Water deficit also appeared to increase absorbance by phenolics in expanding cell walls from 3 to 6 mm behind the tip, where segmental elongation rates in water deficit-treated roots first began to decrease.

The longitudinal and radial distribution of phenolic substances in cell walls of different tissues was investigated in more detail by microscopic assay of the UV-induced autofluorescence produced by phenolics in thin (50 μm) microtome cross sections from along the elongation zone of alcohol-extracted roots. The color

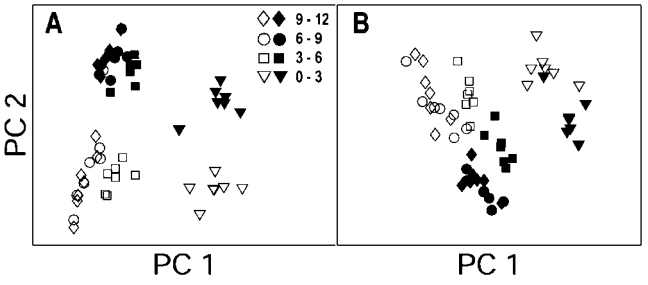

Figure 3. Exploratory PCA confirms stress-induced differences between cell wall FTIR spectra. PCA scores of spectra in the apical region of control and water-stressed roots at 1,800 to 1,600 cm^{-1} (A) and at 1,260 to 1,220 cm^{-1} (B). At these wave numbers, consistent separations are evident between cell wall samples from control (white symbols) and water deficit treatment (black symbols) at all distances from tip.

images in horizontal column A of Figure 4 show that for well-watered control roots, the bright blue-green autofluorescence associated with wall phenolics was virtually absent from cortical and stelar tissues midway along the region 0 to 3 mm behind the tip and was relatively weak at 3 to 6 mm behind the tip. The autofluorescence became somewhat stronger in the inner stelar tissues of the 6-to-9-mm region while fluorescence in the outer epidermal and cortical tissues remained relatively weak.

Horizontal column B shows cross sections excised at equivalent distances from the tips of roots growing under water deficit and viewed at the same intensity of incident UV light. The diameters of these cross sections were relatively reduced, and this is consistent with the thinning of maize roots noted under water deficit regimes (Sharp et al., 1988; Fraser et al., 1990). Although cortical and stelar fluorescence remained weak at 0 to 3 mm from the tip, additional stelar fluorescence (by comparison with well-watered roots) now appeared in the 3-to-6-mm region, i.e. where differences in segmental growth rates also began to appear.

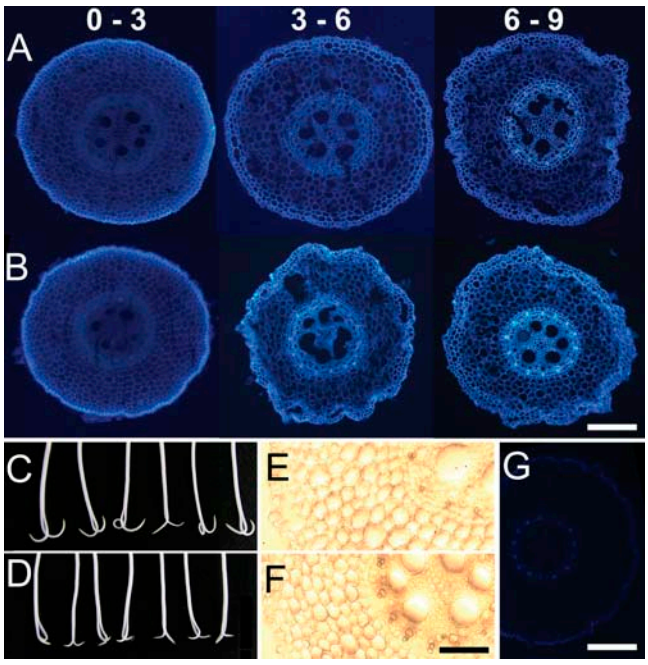

Figure 4. Water deficit effects on cell wall fluorescence, lignin staining, and growth-limiting tissues. Sections (50 μm) were cut with a microtome from around the mid point of regions at indicated distances (millimeters) from the tip of alcohol-extracted cell wall ghosts prepared from well-watered (row A) and water deficit (row B)-treated roots. Root photos (C and D) reveal inward curvature 2 h after longitudinal bisection of elongation zone of live primary roots under control (C) and water deficit treatment (D). Maule-stained free-hand sections 6 to 9 mm from the tip of alcohol-extracted cell wall ghosts were from control roots (E) and water deficit-treated roots (F). Image (G) shows reduced fluorescence in cell walls 6 to 9 mm from tip of water deficit-treated root after 1 h treatment with hot acidic sodium chlorite, which oxidizes phenolics. Horizontal white bars represent 200 μm. Black bar represents 100 μm.

Further stress-induced increases in fluorescence appeared in the region 6 to 9 mm from the tip. The additional stress-associated fluorescence along the region 3 to 9 mm behind the tip was primarily located in vascular areas of the stele corresponding to early metaxylem and surrounding cells. These stress-induced increases in stelar fluorescence were repeatedly observed in microtome sections and earlier, in hand-cut sections.

Weak autofluorescence also occurred along the epidermal regions of the elongation zones of roots under water deficit or control conditions, and treatment-related differences were occasionally observed. These and the treatment-related differences detected by FTIR in bulked cell wall preparations from 0 to 3 mm behind the tip might involve UV fluorescence of phenolic substances trapped in root mucilages secreted by the epidermis (Walker et al., 2003).

Figure 4, C and D, show the inward curvature observed 2 h after bisecting the elongation zone of live roots under control or water deficit conditions (i.e. in PEG). The inward curvature suggests that growth-limiting tissues in the water deficit-treated roots, as in well-watered controls, were located in the inner (stelar) part of the root, rather than the outer cortical tissues and epidermis.

Treatment of cell walls with Maule reagent should produce brown staining in the presence of lignins. Figure 4E shows a section 6 to 9 mm from the root tip of control roots, and Figure 4F shows the equivalently located section from roots under water deficit. Increases in lignin staining were detectable in vascular regions of the stele in water deficit-treated roots. Interestingly, this staining colocalized with stress-induced increases in UV fluorescence. Phloroglucinol-HCl treatment also revealed stress-enhanced lignin staining but only in the walls of a few stelar cells (data not shown).

The phenolic identity of the wall compounds producing UV fluorescence was confirmed by chemical treatments. Treatment of plant cell walls with hot acidic chlorite can oxidize wall-associated phenolics, including those in lignins. Figure 4G shows that most of the autofluorescence in a cell wall cross section taken 6 to 9 mm from the root tip had disappeared after a 1-h chlorite treatment. The same response was observed at other locations along the roots. In addition, the expected enhancement of fluorescence by wall phenolics was observed after exposure of root cell wall cross sections to 0.1 M ammonium hydroxide solution (data not shown; Harris and Hartley, 1976).

DISCUSSION

Water deficit caused by addition of PEG 6000 to the root medium induced reductions in final cell length and progressive reductions in segmental growth rates in basal regions of the elongation zone. These were similar to the results reported by others (Sharp et al.,

1988; Fraser et al., 1990; Pritchard, 1994). The stress-induced reductions in growth were shown to be accompanied by progressive reductions in wall mechanical extensibility of alcohol-treated root segments excised at increasing distances from the root tip (compare with Pritchard et al., 1993; Neumann, 1995; Wu et al., 1996). Thus, our findings help establish the occurrence of a close spatial association between progressively increasing inhibition of segmental growth rates 3 to 6 and 6 to 9 mm behind the tip and progressively decreasing wall extensibility.

It might be argued that the changes induced by water deficit in the region 6 to 9 mm behind the root tip simply reflected the shortening of the effective length of the elongation zone from approximately 9 mm to approximately 6 mm and developmental changes associated with (premature) cell maturation. However, the important question that remains is by what cellular mechanisms does water deficit act to shorten final cell lengths, progressively inhibit segmental growth rates, and decrease the effective length of the root elongation zone?

Since segmental growth rates were not inhibited by water deficit in the region 0 to 3 mm behind the tip, we looked for possible stress-induced changes in wall composition along the region 3 to 9 mm behind the tip. In this region the reductions in segmental growth rates caused by water deficit are initiated (3–6 mm behind the tip) and increased (6–9 mm), as the traversing cells rapidly move toward maturity.

CCR Transcripts

Our finding that transcripts of CCR genes are expressed in the elongation zone of control and water deficit-treated roots is consistent with the idea that water deficit affected lignin metabolism. CCR (EC 1.2.1.44) catalyzes the conversion of hydroxycinnamoyl-CoA thioesters to cinnamaldehydes at the entry point to the monolignol-specific branch of the lignin biosynthetic pathway. Genetic transformations in tobacco (*Nicotiana tabacum*), Arabidopsis, and poplar (*Populus* spp.) have directly confirmed that CCR can affect the amount and composition of lignin accumulated in plant cell walls (Boerjan et al., 2003; Boudet et al., 2003). Because posttranscriptional regulation is possible, the different levels of CCR transcripts in our experiments should not be used to infer actual rates of lignin synthesis. However, the presence of these transcripts does indicate that a potential for lignin synthesis exists in the maize root elongation zone. This conclusion is consistent with the observed accumulation of cell wall phenolics in the root elongation zone as detected by IR and UV approaches and with the wall accumulation of lignin detected by chemical staining. Some further support for the existence of a lignin synthesis infrastructure in the elongation zone is provided by another gene of unknown function (RGG137), which was previously found by us to be preferentially expressed in the elongation zone of maize primary roots and was associated with root growth regulation (Bassani et al., 2004). The gene database subsequently revealed a close analogy to shikimate kinase, which helps generate the aromatic amino acids used in synthesis of lignin.

Water deficit for 1 or 48 h had distinct up-regulatory effects on levels of CCR transcripts, particularly CCR2, which was only weakly expressed in the well-watered roots (compare with Pichon et al., 1998). Increased expression of lignin synthesis genes has been previously associated with the responses of mature tissues to pathogens or mechanical stress (Boerjan et al., 2003; Kimbrough et al., 2004). However, a recent report by Vincent et al. (2005) showed that water deficit treatment can increase the level of caffeate *O*-methyltransferase, an enzyme associated with lignin biosynthesis, in the immature elongating tissues of maize leaves. This report shows the presence and early up-regulation by water deficit, of CCR gene transcripts in the maize root elongation zone.

Increased deposition of lignin would be expected to stiffen the affected cell walls, thereby reducing their extensibility and decreasing rates of cell expansion. It is therefore noteworthy that up-regulated levels of both CCR1 and CCR2 were detectable as early as 1 h after imposing water deficit, i.e. before the onset of significant stress-induced reductions in wall mechanical extensibility. Since the increased expression of CCR transcripts preceded the onset of wall stiffening, a causal relationship between the two events is conceivable. The increased lignin deposition revealed by chemical staining of cell walls in the 6-to-9-mm region of 48-h water-stressed roots directly supports this conclusion. Increased wall deposition of lignin may also help explain limited in vitro response of cell wall extension to acid pH and limited in vivo growth response to acid pH in basal regions of the elongation zone of roots under water deficit, as compared with more apical regions (Wu et al., 1996; Fan and Neumann, 2004).

Spatial Location of Wall Changes in Relation to Root Growth Inhibition

The altered deposition of lignin and wall-bound phenolics induced by water deficit was located primarily in the inner tissues of the root elongation zone. Several reports involving surgical treatments indicate that it is the slower expansion of the inner tissues, as compared with cortical and epidermal tissues, which limits overall rates of maize root elongation under well-watered conditions (compare with Björkman and Cleland, 1991; Pritchard, 1994). The inward curvature observed by us after bisection of the elongation zone of maize roots suggests that the inner tissues continued to have a rate-limiting role under water deficit conditions. Thus, the alterations induced by water deficit in stelar accumulation of lignin might effectively contribute to decreased wall extensibility in the inner tissues and thereby to the inhibition of root elongation.

Wall FTIR Spectra and UV Fluorescence

The digital subtraction of mid-IR spectra of cell walls from control and water-stressed roots provided additional evidence for local and progressive effects of water deficit on the phenolic composition of cell walls. Thus, water deficit caused progressive increases in phenolic-associated FTIR absorbance in expanding root cell walls from regions 3 to 6 and 6 to 9 mm behind the tip, i.e. the regions where growth inhibition was initiated and then progressively increased. The UV-fluorescence microscopy images of cross sections of root cell wall ghosts further confirmed the spatially progressive effects of water deficit. Thus, water deficit resulted in comparative increases in the accumulation in stelar cell walls of the blue-green autofluorescence indicative of phenolics and in chemical staining for lignin. The finding that wall fluorescence was removed by hot acid chlorite and enhanced by ammonium hydroxide further supported the conclusion that water deficit affected the deposition of phenolics (Harris and Hartley, 1976; Rudall and Caddick, 1994). We did not observe increased UV fluorescence in the region of the Casparian band or in exodermal or endodermal tissues, which are known to undergo subero-lignification (compare with Steudle and Peterson 1998; Zeier et al., 1999; Enstone et al., 2003; Karahara et al., 2004). This may be related to lower resolution in our assays and the closeness to the tip of the tissues we assayed.

A possible regulatory role of phenolic wall constituents in the progressive onset of wall hardening and growth inhibition is suggested by the progressive stress-induced increases in levels of wall-bound phenolics indicated by both the FTIR and UV analyses at 3 to 6 and 6 to 9 mm behind the root tip. These increases are consistent with increased ester binding of *p*-coumaric or ferulic acids. Other phenolic constituents such as Tyr, which is a constituent of wall structural proteins and can form dityrosine linkages between them, might also be involved in decreasing wall mechanical extensibility (Fry, 2004). In summary, the UV and FTIR analyses revealed novel spatial associations between accumulation of wall phenolics, decreased wall extensibility, and growth inhibition. However, these techniques could not confirm the specific nature of the substances shown to accumulate in the root cell walls under water deficit or the degree to which they cross-linked load-bearing wall polysaccharides. The link between changes in wall levels of phenolic constituents, wall extensibility, and growth inhibition, is difficult to prove conclusively. Thus, wall ferulic acids could take the form of ester-linked ferulic monomers, which would not be expected to cross-link wall carbohydrates and reduce wall extensibility (though they might perhaps have growth inhibitory effects on the viscosity of the gel matrix in expanding walls). In contrast, ferulic acid dimers or trimers can form interpolymer cross-linkages which could reduce wall extensibility. Even if stress-induced increases in levels of phenolic dimers and trimers could be ascertained, it would still be necessary to show that they actually cross-linked the load-bearing polymers in the expanding walls. For example, it has been noted that ferulic acid trimers might also take the form of intrapolymer loops, and these would be unlikely to affect wall extensibility (Kerr and Fry, 2004).

Although beyond the scope of this report, chemical investigations of the specific types of phenolic molecules accumulated in the cell walls of the stelar tissues of the maize root elongation zone under water deficit are still needed. Selective inhibition of their synthesis by genetic or pharmacological means might then provide conclusive evidence for functional relationships between their accumulation and the local growth inhibition induced by water deficit. Nevertheless, our data provide support for the hypothesis that novel, spatially localized increases in the accumulation of wall-bound phenolics, including lignin, are linked to local root growth inhibition by water deficit and suggest future avenues of enquiry.

Cell Wall Changes and Stress Acclimation

Could the local shifts in root cell wall composition induced by water deficit and the associated inhibition of wall extensibility and root growth contribute in any way to plant acclimation to drying environments? One possibility is that specific inhibition of growth in basal regions of the root elongation zone increases the relative availability of water, minerals, and sugars needed for maintaining minimal growth and survival of the younger cells in more apical regions. Keeping younger cells alive during episodes of intermittent water deficit could facilitate root growth recovery after rehydration.

CONCLUSION

Maize root growth under water deficit is well maintained in the region of the elongation zone situated 0 to 3 mm behind the tip and is progressively inhibited, along with progressive reductions in cell wall extensibility, from 3 to 9 mm behind the tip. This spatially localized growth inhibition may facilitate root acclimation to and survival of drying environments by diverting resources to essential meristemic tissues at the tip. Four lines of interrelated evidence support the hypothesis that alterations in patterns of wall-phenolic accumulation in the root elongation zone may be involved in regulating the inhibition by water deficit of wall extensibility and root growth: (1) Transcripts of two CCR genes involved in lignin biosynthesis were detected in the elongation zone of well-watered and stressed roots; (2) CCR transcript levels increased after only 1 h under water deficit and before reductions in cell wall extensibility, suggesting a possibly causal association; (3) progressive increases in IR absorbance and UV fluorescence, both indicative of wall-bound phenolics, were observed from 3 to

9 mm behind the tips of water deficit-treated roots and colocalized with the progressive inhibition of wall extensibility and growth; and (4) the increases in UV fluorescence and lignin staining induced by water deficit were located primarily to cell walls of inner tissues in the stele, and these tissues appeared to specifically limit root growth rates.

MATERIALS AND METHODS

Plant Growth

Maize seeds (*Zea mays* cv 647) supplied by Galilee Seeds were germinated on moistened filter paper for 4 d and then transferred to hydroponic culture with roots in well-aerated 0.1-strength nutrient solutions under a controlled environment, as in Fan and Neumann (2004). Water deficit was imposed by sequential transfer at 1-h intervals to well-aerated root media containing freshly prepared nutrient solution with the nonpenetrating osmolyte PEG (PEG 6000), plus 0.5 mM $CaCl_2$, at water potentials of −0.1 MPa, −0.2 MPa, −0.3 MPa, −0.4 MPa, and finally −0.5 MPa. For short-term (1 h) experiments used to measure water deficit effects on wall mechanical extensibility and CCR gene expression, seedlings were first sequentially exposed to −0.2 MPa, −0.3MPa, and −0.4 MPa PEG each for 10 min and then to −0.5 MPa PEG for a further 30 min. Segmental growth data were obtained by root marking as in Fan and Neumann (2004).

Lengths of fully elongated cortical cells in hand-cut longitudinal strips from approximately 2 cm behind the growing zone of control or water deficit-treated roots were estimated using images of cell files a few layers outside the vascular cylinder. Images from 14 roots were analyzed. Images were captured using a digital microscope/camera (Olympus, MIC-D/DP01) and the lengths of around 15 clear-cut cells per root were measured by counting pixels at a resolution of 1,105 pixels/mm.

Unless otherwise stated, seedlings were equilibrated under water deficit for 48 h so that all of the cells within and immediately beyond the root elongation zone were representative of cells that developed under water deficit.

Comparative Mechanical Extensibility of Cell Walls

Roots of maize seedlings were grown for 48 h in 0.1-strength Hoagland solution without PEG or with PEG at −0.5 MPa water potential. The apical 20 mm of the roots were then excised and extracted in boiling methanol for 5 min. The resultant cell wall ghosts were stored in methanol. Root samples were hydrated in 0.2 M sodium acetate buffer at pH 4.6 for 15 min. Diameters of the root samples were measured with a low-power microscope and used to determine cross-sectional areas. Individual root samples were secured between two clamps of a Rheoner creep meter (Yamaden RE-33005) so that the extension capacity of root sections at 3 to 6 or 6 to 9 mm from the tip could be assayed (Tanimoto et al., 2000; Hattori et al., 2003). A new root specimen was used for every measurement. The extending region of the root was wetted with buffer solution during the assay. After 5 min of creep extension under a load of 15 g m^{-2} and at a maximum rate of 0.5 mm s^{-1} total in vitro extension was determined as the load-induced increase in segmental length.

CCR mRNA Analysis

Approximately 3 g of root material was excised from the elongation zone starting 1 mm behind the tip of control seedlings and of seedlings exposed to 1 or 48 h of water deficit treatment. The root material was immediately ground in liquid nitrogen. Total cellular RNA was extracted from the ground tissue according to Puissant and Houdebine (1990) and Bassani et al. (2004). RT was carried out using ImProm-II Reverse Transcription system (Promega) and random hexamer primers were used. Gene-specific primers were designed based on two CCR cDNA sequences reported by Pichon et al. (1998) to be expressed in maize roots. The accession numbers in the Nucleotide Sequence Database are X98083 (ZmCCR1) and Y15069 (ZmCCR2). Primers based on regions showing no similarities between the two CCRs were synthesized and primer sequences are given below: ZmCCR1_F (5′-CGTCTCCTCCACCG-ATGCC-3′); ZmCCR1_R (5′-GGCAGATGGCGTCGTAGTCC-3′); ZmCCR2_F (5′-AACAGCAGAGGCGACGACG-3′); and ZmCCR2_R (5′-TCTGTGGGTCCA-GCAGGTCG-3′).

Semiquantitative RT-PCR was carried out using a QuantumRNA18S Internal Standard kit (Ambion) according to the manufacturer's recommendations. The linear range was determined by plotting cycles (18–36) against pixel density of PCR product with equal loading volumes for each sample. Thirty cycles and a 2:8 ratio of 18S primer to competimer was found to be optimal for both genes. The PCR products were separated in a 2% agarose EtBr gel. The pixel density of gel images was read and calculated by MATLAB command. The relative quantity of each sample was obtained as the pixel densities for the gene-specific amplicon divided by the 18S amplicon. In addition, the CCR products of the PCR were cloned into pGEM-easy vector (Promega) and sequenced (Macrogene) to confirm the gene identities.

RNA Gel-Blot Hybridization Analysis

Samples of 20 μg (for CCR1) and 30 μg (for CCR2) of total RNA were separated in 1.2% agarose-formaldehyde gels, transferred to Amersham Hybond-N nylon membranes, and cross-linked by UV radiation. Hybridization probes were made by cloning the PCR fragments into pGEM-easy vector, and the gene identity was confirmed by its sequence. Specific primers were used to amplify the sequences. Labeling was generated by random priming in the presence of [a-^{32}P] dCTP (Amersham). Prehybridization, hybridization, and washing were conducted according to Sambrook et al. (1989). The membrane was visualized after 12 h in a phosphor imager (Fujifilm image reader FLA-5000).

FTIR Spectra of Root Cell Walls

Maize roots were grown for 48 h in 0.1-strength Hoagland solution ± 0.5 MPa PEG 6000. Roots were excised at about 2 cm from the tip. The 2-cm sections were plunged into 50% ethanol at 85°C for 10 min. The roots were subsequently extracted in 80% ethanol at 85°C for 10 min and absolute ethanol at 85°C for 10 min. The resultant root cell wall ghosts were then cut into sections 0 to 3, 3 to 6, 6 to 9, and 9 to 12 mm from the tip and stored in absolute ethanol at 4°C.

Prior to use, root sections were removed from alcohol and dried at 45°C for 0.5 h. Aliquots of 2 mg were then ground in a mortar with 200 mg of pure desiccated KBr to produce a uniform powder. The mixture was transferred to a 13-mm die and pressure at approximately 9,000 kg was applied for 2 min under continuous evacuation. This produced a 13-mm diameter and 1-mm thick disc as described by Stuart (1997).

A FTIR spectrometer (Vector 22, Bruker Optic) was used to obtain the IR spectra. The spectrometer was equipped with a mercury-cadmium-telluride detector. Each disc was scanned 32 times, and the average absorbance spectrum in the 4,000 to 400 cm^{-1} range was recorded. The spectrum was baseline corrected and area normalized in the region 2,000 to 800 cm^{-1} by using OPUS-NT spectroscopic software (version 3, Bruker Optic). Results of six replicate experiments were combined to produce average spectra for each section of the root.

Differences between spectra of walls of roots from control and water deficit treatments were investigated using PCA, a mathematical procedure commonly used for data reduction and/or data classification (e.g. Jackson, 1991; Chen et al., 1998). The information contained in the original data is condensed into a small number of so-called scores, which are the projections of the original data onto new reference axes (so-called principal component or loadings). Most of the information (variance) contained in the original data is reflected in the first few scores and loadings. Similarity/dissimilarity in the original data can be investigated by plotting these scores against each other and identifying score clusters. In this study, when PCA was applied to two distinct intervals of the spectrum (1,260–1,220 cm^{-1} and 1,800–1,700 cm^{-1}), more than 98% of the variance contained in the original spectra was explained by the first two scores and loadings.

Cell Wall Microscopy

Root cell wall ghosts were prepared by hot alcohol extraction. Sections 1 mm long were then hand cut from the middle of regions 0 to 3, 3 to 6, 6 to 9, and 9 to 12 mm from the tip. For chlorite treatment, sections were transferred to 0.34 M $NaClO_2$ in 65 mM acetic acid at 65°C for 1 h, rinsed in distilled water several times, and stored in ethanol (Carpita et al., 2001). Root sections were fixed for 48 h in phosphate-buffered saline (pH 7.4) containing 3.7% (w/v) formaldehyde (Zeier et al., 1999). The sections were then placed on aluminum

foil, coated with a thin layer of embedding medium, Tissue-Tek OCT (Sakura Finetek), and frozen in liquid nitrogen. Frozen sections were placed on the specimen block of a cryo-stat microtome (Jung Frigocut 2800 N, Leica Instruments) at −20°C together with a few drops of embedding medium. Cross sections 50 μm thick were cut from the middle of each segment, transferred to glass slides, and mounted in glycerol/water (1:1; v/v). Images of root autofluorescence were viewed using a Leica DMIRE2 Inverted Research Microscope (Welzlar) equipped with a Leica DC 300 FX camera (Leica Microsystems, Digital Imaging). A 359-nm UV excitation line isolated using a filter cube was reflected onto the root samples and emitted light was used to generate the image. To obtain identical conditions the automatic contrast, gamma, and exposure controls were switched to standard conditions (gain 1; black and white balance 0,100; gamma, 1). Optimal resolution for viewing root sections was obtained with the exposure time adjusted to 350 milliseconds.

For staining experiments, root cross sections were hand cut from the middle of the region 6 to 9 mm behind the tip of alcohol-extracted and rehydrated cell wall ghosts prepared from well-watered and water deficit-treated roots. These were stained using Maule reagent as described by Chapple et al. (1992). The sections were treated with 0.5% $KMnO_4$ for 10 min. Sections were then rinsed with water, treated with 10% HCl for 5 min, rinsed with water, mounted in concentrated NH_4OH, and examined under bright-field microscopy.

Received October 20, 2005; revised October 20, 2005; accepted November 21, 2005; published December 29, 2005.

LITERATURE CITED

Bassani M, Neumann PM, Gepstein S (2004) Differential expression profiles of growth-related genes in the elongation zone of maize primary roots. Plant Mol Biol **56:** 367–380

Birnbaum K, Shasha DE, Wang JY, Jung JW, Lambert GM, Galbraith DW, Benfey PN (2003) A gene expression map of the Arabidopsis root. Science **302:** 1956–1960

Björkman T, Cleland RE (1991) The role of extracellular free-calcium gradients in gravitropic signalling in maize roots. Planta **185:** 379–384

Boerjan W, Ralph J, Baucher M (2003) Lignin biosynthesis. Annu Rev Plant Biol **54:** 519–546

Boudet AM, Kajita S, Grima-Pettenati J, Goffner D (2003) Lignins and lignocellulosics: a better control of synthesis for new and improved uses. Trends Plant Sci **8:** 576–581

Boyer JS (1982) Plant productivity and environment. Science **218:** 443–448

Carpita NC (1996) Structure and biogenesis of the cell walls of grasses. Annu Rev Plant Physiol Plant Mol Biol **47:** 445–476

Carpita NC, Defernez M, Findlay K, Wells B, Shoue DA, Catchpole G, Wilson RH, McCann MC (2001) Cell wall architecture of the elongating maize coleoptile. Plant Physiol **127:** 551–565

Carpita NC, McCann MC (2002) The functions of cell wall polysaccharides in composition and architecture revealed through mutations. Plant Soil **247:** 71–80

Chapple CCS, Vogt T, Ellis BE, Somerville CR (1992) An Arabidopsis mutant defective in the general phenylpropanoid pathway. Plant Cell **4:** 1413–1424

Chen L, Carpita NC, Reiter WD, Wilson RH, Jeffries C, McCann MC (1998) A rapid method to screen for cell-wall mutants using discriminant analysis of Fourier transform infrared spectra. Plant J **16:** 385–392

Cosgrove DJ (2000) Loosening of plant cell walls by expansins. Nature **407:** 321–326

Degenhardt B, Gimmler H (2000) Cell wall adaptations to multiple environmental stresses in maize roots. J Exp Bot **51:** 595–603

Dolan L, Davies J (2004) Cell expansion in roots. Curr Opin Plant Biol **7:** 33–39

Enstone DE, Peterson CA, Ma FS (2003) Root endodermis and exodermis: structure, function, and responses to the environment. J Plant Growth Regul **21:** 335–351

Fan L, Neumann PM (2004) The spatially variable inhibition by water deficit of maize root growth correlates with altered profiles of proton flux and cell wall pH. Plant Physiol **135:** 2291–2300

Fraser TE, Silk WK, Rost TL (1990) Effects of low water potential on cortical cell length in growing regions of maize roots. Plant Physiol **93:** 648–651

Fry SC (1979) Phenolic components of the primary cell wall and their possible role in the hormonal regulation of growth. Planta **146:** 343–351

Fry SC (1986) Cross-linking of matrix polymers in the growing cell walls of angiosperms. Annu Rev Plant Physiol **37:** 165–186

Fry SC (2004) Primary cell wall metabolism: tracking the careers of wall polymers in living plant cells. New Phytol **161:** 641–675

Harris PJ, Hartley RD (1976) Detection of bound ferulic acid in the cell walls of the Gramineae by ultraviolet fluorescence microscopy. Nature **259:** 508–510

Hattori T, Inanaga S, Tanimoto E, Lux A, Luxova M, Sugimoto Y (2003) Silicon-induced changes in viscoelastic properties of sorghum root cell walls. Plant Cell Physiol **44:** 743–749

Jackson JE (1991) A User's Guide to Principal Components. John Wiley & Sons, New York

Jung HJG (2003) Maize stem tissues: ferulate deposition in developing internode cell walls. Phytochemistry **63:** 543–549

Kamisaka S, Takeda S, Takahashi K, Shibata K (1990) Diferulic and ferulic acid in the cell wall of *Avena* coleoptiles: their relationships to mechanical properties of the cell wall. Physiol Plant **78:** 1–7

Karahara I, Ikeda A, Kondo T, Uetake Y (2004) Development of the Casparian strip in primary roots of maize under salt stress. Planta **219:** 41–47

Kerr EM, Fry SC (2004) Extracellular cross linking of xylan and xyloglucan in maize cell suspension cultures: the role of oxidative phenolic coupling. Planta **219:** 73–83

Kimbrough JM, Salinas-Mondragon R, Boss WF, Brown CS, Sederoff HW (2004) The fast and transient transcriptional network of gravity and mechanical stimulation in the Arabidopsis root apex. Plant Physiol **136:** 2790–2805

MacAdam JW, Grabber JH (2002) Relationship of growth cessation with the formation of diferulate cross-links and p-coumaroylated lignins in tall fescue leaf blades. Planta **215:** 785–793

Masuda Y (1990) Auxin-induced cell elongation and cell wall changes. Bot Mag Tokyo **103:** 345–370

Neumann PM (1995) The role of cell wall adjustment in plant resistance to water deficits. Crop Sci **35:** 1258–1266

Neumann PM, Azaizeh H, Leon D (1994) Hardening of root cell walls: a growth inhibitory response to salinity stress. Plant Cell Environ **17:** 303–309

Passardi F, Penel C, Dunand C (2004) Performing the paradoxical: how plant peroxidases modify the cell wall. Trends Plant Sci **9:** 534–540

Pichon M, Courbou I, Beckert M, Boudet AM, Grima-Pettenati J (1998) Cloning and characterization of two maize cDNAs encoding cinnamoyl-CoA reductase (CCR) and differential expression of the corresponding genes. Plant Mol Biol **38:** 671–676

Pritchard J (1994) The control of cell expansion in roots. New Phytol **127:** 3–26

Pritchard J, Hetherington PR, Fry SC, Tomos AD (1993) Xyloglucan endotransglycosylase activity, microfibril orientation and the profiles of cell wall properties along growing regions of maize roots. J Exp Bot **44:** 1281–1289

Puissant C, Houdebine LM (1990) An improvement of the single step method of RNA isolation by acid guanidinium thiocyanat phenol-chloroform extraction. Biotechniques **8:** 148–149

Ralph J, Grabber JH, Hatfield RD (1995) Lignin-ferulate cross-links in grasses: active incorporation of ferulate polysaccharide esters into ryegrass lignins. Carbohydr Res **279:** 167–178

Rayle DL, Cleland RE (1992) The acid growth theory of auxin-induced cell elongation is alive and well. Plant Physiol **99:** 1271–1274

Rose JKC, Saladié M, Catalá C (2004) The plot thickens: new perspectives of primary cell wall modification. Curr Opin Plant Biol **7:** 296–301

Rudall PJ, Caddick LR (1994) Investigation of the presence of phenolic compounds in monocotyledonous cell walls, using UV fluorescence microscopy. Ann Bot (Lond) **74:** 483–491

Sambrook J, Fritsch EF, Maniatis T (1989) Molecular Cloning: A Laboratory Manual, Ed 2. Cold Spring Harbor Laboratory Press, Cold Spring Harbor, NY

Schopfer P, Lapierre C, Nolte T (2001) Light-controlled growth of the maize seedling mesocotyl: mechanical cell-wall changes in the elongation zone and related changes in lignification. Physiol Plant **111:** 83–92

Séné CFB, McCann MC, Wilson RH, Grinter R (1994) Fourier-transform Raman and Fourier-transform infrared spectroscopy: an investigation of five higher plant cell walls and their components. Plant Physiol **106:** 1623–1631

Sharp RE, Poroyko V, Hejlek LG, Spollen WG, Springer GK, Bohnert HJ, Nguyen HT (2004) Root growth maintenance during water deficits: physiology to functional genomics. J Exp Bot **55:** 2343–2351

Sharp RE, Silk WK, Hsaio TC (1988) Growth of the maize primary root at low water potentials. 1. Spatial distribution of expansive growth. Plant Physiol **87:** 50–57

Sinclair TR, Muchow RC (2001) System analysis of plant traits to increase grain yields on limited water supplies. Agron J **93:** 263–270

Spollen WG, Sharp RE (1991) Spatial distribution of turgor and root growth at low water potentials. Plant Physiol **96:** 438–443

Steudle E, Peterson CA (1998) How does water get through roots? J Exp Bot **49:** 775–788

Stuart B (1997) Sampling methods. *In* DJ Ando, ed, Biological Application of Infrared Spectroscopy. John Wiley & Sons, New York, pp 35–58

Taiz L (1984) Plant cell expansion: regulation of cell wall mechanical properties. Annu Rev Plant Physiol **35:** 585–657

Tanimoto E, Fujii S, Yamamoto R, Inanaga S (2000) Measurement of viscoelastic properties of root cell walls affected by low pH in lateral roots of *Pisum sativum* L. Plant Soil **226:** 21–28

Van der Weele CM, Jiang HS, Palaniappan KK, Ivanov VB, Palaniappan K, Baskin TI (2003) A new algorithm for computational image analysis of deformable motion at high spatial and temporal resolution applied to root growth: roughly uniform elongation in the meristem and also, after an abrupt acceleration, in the elongation zone. Plant Physiol **132:** 1138–1148

Vincent D, Lapierre C, Pollet B, Cornic G, Negroni L, Zivy M (2005) Water deficits affect caffeate *O*-methyltransferase, lignification, and related enzymes in maize leaves: a proteomic investigation. Plant Physiol **137:** 949–960

Walker TS, Bais HP, Grotewold E, Vivanco JM (2003) Root exudation and rhizosphere biology. Plant Physiol **132:** 44–51

Wu Y, Sharp RE, Durachko DM, Cosgrove DJ (1996) Growth maintenance of the maize primary root at low water potentials involves increases in cell wall extension properties, expansin activity, and wall susceptibility to expansins. Plant Physiol **111:** 765–772

Yamamoto R (1996) Stress relaxation property of the cell wall and auxin-induced cell elongation. J Plant Res **109:** 75–84

Zeier J, Ruel K, Ryser U, Schreiber L (1999) Chemical analysis and immunolocalisation of lignin and suberin in endodermal and hypodermal/rhizodermal cell walls of developing maize (Zea mays L.) primary roots. Planta **209:** 1–12